

Detachment-Influenced Transport of an Adhesion-Deficient Bacterial Strain within Water-Reactive Porous Media

MEIPING TONG, XIQING LI,
CHRISTINA N. BROW, AND
WILLIAM P. JOHNSON*

*Department of Geology and Geophysics, University of Utah,
Salt Lake City, Utah 84112-0111*

Bacteria and carboxylate-modified microsphere transport experiments were performed in glass bead packed columns in order to examine the distribution of retained colloids on the sediment. Solution pH was allowed to vary from 6.0 to 9.4 across the length of the column (20 cm) in order to examine potential effects of solution chemistry on the retained profiles. Both the microspheres and the bacteria showed retained profiles that deviated strongly from log-linear behavior expected from a spatially invariant colloid deposition rate coefficient. Deviation for the microspheres was in the form of steeper-than-expected decreases in retained concentrations with distance from source. Deviation for the bacteria was in the form of maximum retained concentrations that were located down-gradient from the column inlet. Subsidiary experiments with varying elution times showed that detachment during elution moved the peak of mass of retained bacteria down-gradient of the column inlet; however, the disproportional translation of the peak of mass relative to elution time indicated that processes operating during injection produced the initial down-gradient translation of peak concentrations of retained cells.

Introduction

Theories governing colloid transport in porous media characterize colloid deposition rate coefficients as being invariant with transport distance; e.g. clean bed filtration theory (1–3). For a system in which colloid deposition rate coefficients are invariant with transport distance, one observes log linear decreases in mobile and retained colloid concentrations with increasing distance from source (log-linear profiles).

Changes in colloid deposition rate coefficients with distance are increasingly reported, the most common being decreases in colloid deposition rate coefficient with transport distance, as evidenced by concentrations of retained colloids that decrease with distance from source faster than the log-linear rate expected from a spatially invariant deposition rate coefficient (hyperexponential decrease).

Hyperexponential decreases have been widely reported in experiments examining the transport of bacteria in the laboratory (4–7), bacteria in the field (8–10), protists in the laboratory (11), viruses in the laboratory (12, 13), viruses in

the field (14–18), and microspheres in the laboratory (19, 20). In the biological colloid literature, the observed hyperexponential decrease has been largely attributed to distributions in surface properties among the microbial population (4–7, 13) and the collector surfaces (11, 17, 18).

In the nonbiological colloid literature, hyperexponential decreases of retained microsphere concentrations have also been recently observed (19, 20). In the experiments of Bradford et al. (19) this was attributed to straining on the basis that deposition rates increased directly with increasing colloid size. In contrast, Li et al. (20) concluded that straining may play a significant role only at low ionic strength and determined that this behavior could indeed be attributed to a distribution in surface properties among the microsphere population. More recently, Li et al. (21) showed that other forms of deviation from log-linear behavior may occur, specifically, the center of mass of the retained colloids may occur some distance down-gradient of the column inlet, even in the absence of significant colloid detachment.

Colloid deposition rate coefficients can also change temporally due to blocking (22–27) and filter ripening (23, 26) effects. However, this paper will restrict the analysis to apparent spatial changes in colloid deposition rate coefficients in the absence of these temporal effects.

Colloid detachment has mostly been considered negligible during filtration, except under conditions where retained colloids are subjected to a perturbation in flow or solution chemistry (28–32). The assumption of negligible colloid detachment is based on the relatively low rates of colloid re-entrainment following breakthrough of an injected pulse. However, some investigators have suggested (based on numerical simulations) that in some contexts a high degree of reversible attachment might be observed and might lead to significant down-gradient translation of the retained colloids (10, 33).

Contexts in which changes in solution chemistry along the flowpath might be of concern include riverbank filtration, a process in which impaired river water is treated by passage through riverbank sediments during transit to a water supply well (34). Riverbank filtration requires maintenance of sufficient colloid deposition rates to ensure treatment of the water to a specified level. However, water–rock interaction during transit to the well may change water chemistry to an extent governed by constituent mineral solubilities under the chemical conditions of the system (35). The general processes of water–rock equilibration can be expected to yield increased pH and increased ionic strength (35).

Since environmental conditions involve colloids and sediment surfaces that each display bulk negative charge (electrostatically repulsive); increases in ionic strength would be expected to yield increased particle retention (36–44), via compression of the electrostatic double layer of counterions that balance the surface charge of the colloids and the sediment. Increases in pH would be expected to yield greater bulk negative surface charge and decreased particle retention (45–50). However, the opposite trend has also been reported even for negatively charged bacteria (40), likely due to the complex chemistries associated with bacterial extracellular polymers, which include polysaccharides, proteins, and nucleic acids (51). Hence, as water chemistry changes due to water–rock interaction, colloid deposition rates may be expected to increase or decrease depending on the specific effects of changes in pH and ionic strength, which themselves will depend on the surface and aquatic chemical attributes of the system.

* Corresponding author phone: (801)581-5033; fax: (801)581-7065; e-mail: wjohnson@mines.utah.edu.

The purpose of this paper is to demonstrate changes in colloid (microsphere and bacteria) retention rates with distance in reactive porous media. The porous media (glass beads) was chosen such that the dominant change in water chemistry during transit was an increase in pH from 6.0 to 9.4 from the influent to the effluent ends of the column. A steady-state breakthrough plateau was achieved in all experiments, indicating a lack of temporal changes in deposition rate coefficient. The steady-state breakthrough plateau provided no evidence of the surprising distributions of retained colloid concentrations that were achieved on the sediment column. Significant, and in some cases drastic, deviation from theory-based expectations were observed. The profiles of retained microspheres showed faster than log-linear decreases in retained concentrations with distance from the inlet. The profiles of retained bacteria showed maximum retained concentrations down-gradient from the inlet. Detachment was shown to contribute to the observed profiles of retained bacteria. These deviations carry important implications for filtration processes in many contexts, including riverbank filtration.

Materials and Methods

Microsphere Preparation. The microspheres used in column experiments were spherical fluorescent carboxylate-modified polystyrene latex microspheres (1.1 μm diameter, 0.18 meq g^{-1} surface charge density). The microsphere stock suspensions (Molecular Probes, Inc., Eugene, OR) were used as received with a particle concentration of $2.7 \times 10^{10} \text{ mL}^{-1}$ and 2 mM of NaN_3 as the antibacterial agent. Prior to injection, an aliquot of stock suspensions was diluted to achieve an influent concentration (C_0) of $1.35 \times 10^7 \pm 10\%$ particles mL^{-1} in salt solution with the desired ionic strength. The influent concentration of each experiment was normalized to 1.35×10^7 particles mL^{-1} to allow comparison between experiments.

Bacteria Preparation. Bacteria used in the experiments were *Comamonas* DA001, an adhesion-deficient, nonmotile strain isolated from a site near Oyster, VA. DA001 was approximately 1.1 μm by 0.3 μm in size and has a density equal to 1.06 g cm^{-3} (10). Cells were grown at room temperature (22 °C) overnight while shaking at 120 rpm in filter-sterilized basal salts medium (BSM), supplemented with filter-sterilized 0.012 M sodium lactate. BSM consisted of 4.25 g of $\text{K}_2\text{HPO}_4 \cdot 3\text{H}_2\text{O}$, 1 g of $\text{NaH}_2\text{PO}_4 \cdot \text{H}_2\text{O}$, 2 g of NH_4Cl , 0.123 g of $\text{N}(\text{CH}_2\text{CO}_2\text{Na})_3 \cdot \text{H}_2\text{O}$, 0.2 g of $\text{MgSO}_4 \cdot 7\text{H}_2\text{O}$, 0.012 g of $\text{FeSO}_4 \cdot 7\text{H}_2\text{O}$, 0.003 g of $\text{MnSO}_4 \cdot \text{H}_2\text{O}$, 0.003 g of $\text{Zn SO}_4 \cdot 7\text{H}_2\text{O}$, and 0.001 g of $\text{CoCl}_2 \cdot 6\text{H}_2\text{O}$ dissolved in 1000 mL of Milli-Q water and autoclaved at 121 °C. Cells were reinoculated under the same conditions upon reaching visible light absorbance ($\lambda = 660 \text{ nm}$) equal to 0.6 (Beckman DU 650, Fullerton, CA) and were harvested by centrifugation (10,000 g for 10 min at 4 °C) upon reaching the stationary phase (~12 h) with ABS_{660} about 1.2. Cells were resuspended in Narrow Channel artificial groundwater (NCAGW). NCAGW consisted of 60 mg of $\text{MgSO}_4 \cdot 7\text{H}_2\text{O}$, 10 mg of KNO_3 , 60 mg of NaHCO_3 , 60 mg of $\text{CaCl}_2 \cdot 2\text{H}_2\text{O}$, 70 mg of $\text{Ca}(\text{NO}_3)_2 \cdot 4\text{H}_2\text{O}$, 25 mg of $\text{CaSO}_4 \cdot 2\text{H}_2\text{O}$, and 0.4 mg of NaH_2PO_4 dissolved in 1000 mL of deionized water, and 2 N HCl was used to adjust the pH to 6.0. The centrifugation-resuspension process was repeated three times. Cells were subsequently starved at 15 °C for 48–72 h (shaking at 60 rpm) to stabilize surface properties. Following starvation, cells were centrifuged and resuspended three times as described above. Cells were stained using DAPI (4',6-diamidino-2-phenylindole) (Pierce, Rockford, IL) at a concentration of 25 $\mu\text{g mL}^{-1}$ with gentle vortexing for 20 min. Following staining, cells were centrifuged and resuspended three times in NCAGW with the desired ionic strength (NaCl). Direct counts on an epifluorescence microscope were used to determine the stock concentration, which was diluted

to obtain the target influent concentration of $2.0 \times 10^4 \pm 50\%$ cells mL^{-1} , to reflect the relatively low concentrations of cells in environmental waters. The influent concentrations of different experiments were normalized to 1.0×10^4 cells mL^{-1} for ease in comparison.

Porous Media. Spherical soda lime glass beads with sizes ranging from 300 to 417 μm (Cataphote Inc. Jackson, MS) were used as the porous media for microsphere transport experiments. Bead sizes ranging from 417 to 600 μm (Cataphote Inc. Jackson, MS) were used as the porous media for bacteria transport experiments.

The glass beads were first rinsed sequentially with acetone and hexane for 5 min, respectively, and then soaked with concentrated HCl for about 12 h. The beads were rinsed with deionized water until the conductivity was negligible relative to 0.1 M NaOH, as determined using a conductivity meter (Conductance/TDS Model 72, Engineered Systems & Design, Newark, DE). The glass beads were soaked with 0.1 M NaOH for another 12 h, followed by repeated rinsing with Milli-Q water (Millipore Corp. Bedford, MA) until the ionic strength of the glass beads was negligible relative to the experimental ionic strength. The glass beads were dried in an oven (105 °C).

Column Experiments. Cylindrical Plexiglass columns (20 cm long, 3.81 cm inner diameter) were dry-packed after the glass beads were dried and cooled. Packing was performed by adding glass beads in small increments (~2 cm) with mild vibration of the column. Two 60 mesh stainless steel screens (Gerard Daniel Worldwide, Hanover, PA) were placed at each end of the column. To spread the flow upon entry into the column, 3.5 g of coarse sand (>30 mesh, cleaned as described above) were added to the top of the influent screen, forming a 2 mm-thick layer that was covered by another screen. The mass of packed glass beads in each column differed by less than 2 g. The porosity of the packed glass beads was 0.38, as determined by weighing before and after saturating the column and dividing aqueous phase volume derived from the mass difference by the total volume of the column.

The packed columns were purged with CO_2 for 25 min to replace air (since CO_2 is soluble in water) and were pre-equilibrated with salt solution at the desired ionic strength (NaCl) for 6 pore volumes. The 6-pore volume preequilibration required 16 h. Prior to preequilibration, a discontinuous air film was observed on the wall of the column. The air film was removed by the end of the first pore volume of preequilibration, as determined using a magnifying glass. One pore volume was equal to 83 mL (determined gravimetrically). After preequilibration, 3 pore volumes of colloid suspension were injected, followed by 7 pore volumes (14 and 21 for longer elution) of salt solution (without microsphere/ bacteria) at the same ionic strength. Ionic strength conditions varied over the range 0.006–0.02 M for microsphere transport experiments and 0.0038–0.02 M for bacteria experiments.

In the absence of buffer, the solution pH increased from 6.0 to 9.4 from the influent to the effluent end of the column, due to dissolution of Na_2O and CaO on the glass bead surfaces (52). Since this pH range reflects the range observed between surface water and groundwater (35), unbuffered solutions offered a convenient means of representing solution chemistry changes along a representative flowpath from surface to groundwater. Flow rate was varied to produce pore water velocities ranging between 2 and 8 m day^{-1} , since detachment was implicated as a contributor to the shape of the retained profiles (as described below). Parallel experiments examining effluent pH showed that the same change from influent to effluent (6.0 to 9.4) was obtained for all three flow rates. Furthermore, these experiments showed that the pH of the effluent was constant (9.4) throughout the course of each

experiment. The reservoir containing the bacteria solution also contained tritium as a tracer at a concentration of 160 $\mu\text{Ci L}^{-1}$.

The bacterial transport experiments were run with autoclaved water in the refrigerator at temperature 8 °C to limit or prevent possible growth and death of bacteria during the experiment.

Sample Collection and Analysis. Samples from the column effluent were collected every 0.037 pore volumes (3.1 mL) in sterile 5 mL polypropylene culture tubes (VWR, West Chester PA) using a fraction collector (CF-1, Spectrum Chromatography, Houston TX). The collected bacteria samples were preserved using formaldehyde (1%) and were refrigerated at 4 °C until analysis (within several days).

Following completion of the experiment, the sediment was extruded from the column and dissected into 10 segments (each 2 cm long). The retained particles were desorbed by placing the sediment segments into specific volumes of Milli-Q water. The effluent samples and the supernatant samples from the recovery of retained (desorbed) microspheres were analyzed with flow cytometry (BD FACScan, Becton Dickinson & Co., Franklin Lakes, NJ). Details were given by Li et al. (20). The effluent samples and the retained samples of DA001 were analyzed using a Bio-Ferrograph (2100, Institute Guilfoyle, Belmont, MA), as described below.

Enumeration of DA001 in effluent and desorption samples was accomplished using the bioferrographic technique developed by Zhang and Johnson (53). The method used selective immuno-magnetic tagging to ferrographically separate the DA001 cells from solution. A Bioferrograph (Institute Guilfoyle, Belmont MA) was used to draw a sample volume through a small chamber over a glass substrate that was positioned over a magnetic interpolar gap. The magnetic field was strongest at the gap, and magnetically susceptible particles were deposited on the substrate.

The method involved combining 160 μL of fluorescein isothiocyanate (FITC)-conjugated polyclonal rabbit antibodies to DA001 (Rockland Laboratories, Gilbertsville, PA), 40 μL of goat-anti rabbit paramagnetic beads (50 nm diameter, Miltenyi Biotec, Auburn CA), and 0.5 mL of Milli-Q water and vortexing the solution for 15 min at room temperature (22 °C). Antibodies which were not attached to the paramagnetic beads were removed using Mini-MACS separation columns (Miltenyi Biotec, Auburn CA) according to the manufacturer's protocol.

Bioferrographic separation has an unusually high resolution, with a quantitation limit of about 20 cells per mL (10, 53, 54). Because the method involves direct counting, high concentration samples must be diluted to yield cell concentration ranging from 100 to 1000 cells per mL. 50 μL of 2 M NaCl was also added to sample aliquots to increase the ionic strength to approximately 150 mM, which was conducive to proper conformation of the antibody. Following dilution, paramagnetic bead-antibody solution (100 μL) was added to a 0.5 mL aliquot of cell suspension, which was then vortexed at room temperature (22 °C) for 15 min.

The aliquots were introduced into the Bioferrograph and drawn through the chambers at a rate of 0.008 mL min⁻¹. Once the aliquots had passed through the chambers, the glass substrates were dismounted and glued onto glass slides using Prolong anti-fade mounting media (Molecular Probes, Eugene, OR). These slides were then enumerated using FITC fluorescence on an epifluorescence microscope (Nikon, Tokyo, Japan).

One in every 5 samples was a blank to guard against contamination during the bioferrographic procedure. Standards were run every 16 samples to ensure that complete recovery by antibodies was achieved. Since standards decayed

TABLE 1. Experimental Conditions, Mass Balances, and Model Parameters for Simulations Using the Particle Tracking Model (55)

colloids	ionic strength (M)	flow velocity (m day ⁻¹)	mass recovery %	retained %	k_f (h ⁻¹)	k_r (h ⁻¹)	f_r
microspheres	0.006	4	99.1	17.1	0.15	0.33	0.26
	0.01	4	96.6	34.4	0.39	0.23	0.08
	0.02	4	109.5	67.2	0.71	0.45	0.03
	0.006	2	107.8	34.5	0.16	0.12	0.25
	0.006	8	102.0	8.5	0.13	3.20	0.20
	0.0038	4	105.1	13.9	0.20	0.10	0.98
bacteria	0.01	4	101.1	70.6	1.50	0.08	0.80
	0.02	4	101.9	71.0	1.51	0.08	0.40
	0.02	2	92.1	88.5	1.62	0.05	0.28
	0.02	8	73.66	23.0	1.30	0.25	0.90

over time, the measured decay rate was used to adjust analytical results to account for this known decay rate of the samples.

The area under the breakthrough-elution curve was integrated to yield the number of microspheres or bacteria that exited the column. The colloids recovered from all segments of the sediment were summed to determine the total number of retained colloids. The overall recovery (mass balance) of colloids was determined by summing the numbers of retained colloids and colloids that exited the column. The overall recovered number of colloids was divided by the number of injected colloids to express the mass balance as a percentage.

Particle Tracking Model. Breakthrough curves and retained profiles were simulated using a numerical model based on an advection-dispersion governing equation that included removal from, and re-entrainment to, the aqueous phase

$$\frac{\partial C}{\partial t} = -v \frac{\partial C}{\partial x} + D \frac{\partial^2 C}{\partial x^2} - k_f C + \frac{\rho_b}{\theta} k_r S_r \quad (1)$$

where C is the concentration of colloids in the aqueous phase (colloids per unit volume of fluid), t is the travel time, x is the travel distance, v is the fluid velocity, D is the dispersion coefficient of the colloids, θ is the porosity, ρ_b is the bulk density of sediment, and k_f and k_r are rate coefficients for colloid deposition to, and re-entrainment (detachment) from, the solid phase, respectively. S_r is the reversibly retained colloid concentration on the solid phase (colloids per unit mass of sediment) and can be further expressed as

$$S_r = S f_r \quad (2)$$

where S is the total deposited colloid concentration and f_r is the fraction of reversibly retained colloids.

A one-dimensional discrete random-walk particle-tracking model was used to solve eq 1 under the conditions of the column experiments. This model has been previously applied to simulate bacteria transport with emphasis on characterization of long-term detachment tailing (10), size exclusion (55), and more recently, observed deviations from log-linear profiles of retained microspheres on glass beads (20) and quartz sand (21). De-coupling of S_r and k_r occurs during probabilistic implementation of k_r . Detailed description of the model is provided in these references.

Results

Mass Balances. Mass recoveries (total from effluent and sediment) for microsphere transport experiment were virtually all between 96% and 110%. Mass recoveries for bacteria transport experiments (total from effluent and sediment) were between 73% and 105% (Table 1), with the majority between 89% and 105%.

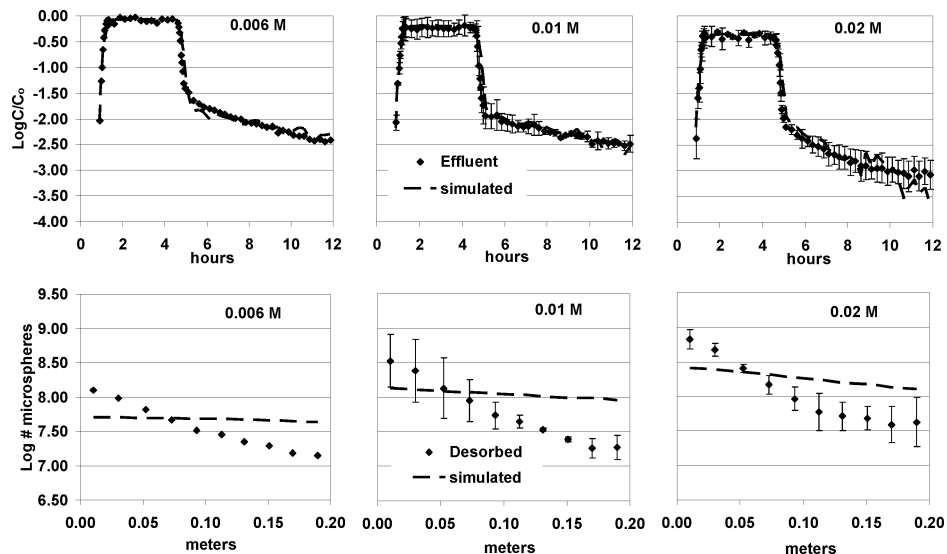


FIGURE 1. Ionic strength series for $1.1 \mu\text{m}$ microspheres at flow rate $= 4 \text{ m day}^{-1}$, showing effluent breakthrough-elution curves (top) and retained (desorbed) profiles (bottom). Error bars represent standard deviations in results from replicate experiments ($n = 2-4$). Simulations use the particle tracking model with a single deposition rate coefficient (k_d) (dashed lines).

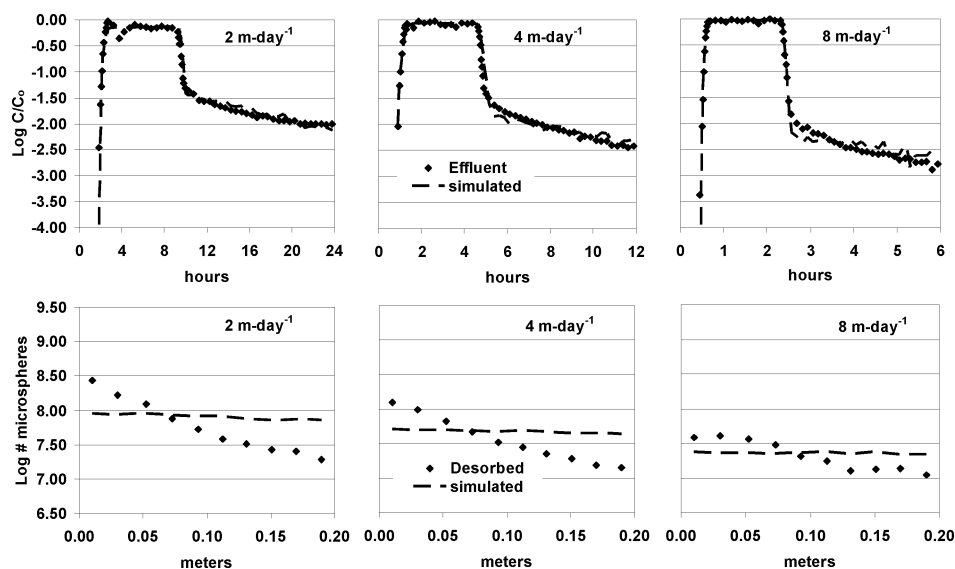


FIGURE 2. Flow rate series at ionic strength $= 0.006 \text{ M}$, for $1.1 \mu\text{m}$ microspheres showing effluent breakthrough-elution curves (top) and retained (desorbed) profiles (bottom). Simulations are shown from the particle tracking model using a single deposition rate coefficient (k_d) (dashed lines).

Breakthrough-Elution Curves. The steady-state breakthrough plateaus for both the microspheres and bacteria were, for the most part, flat, indicating temporal constancy of the deposition rate coefficient (negligible blocking or ripening) during the course of the majority of the experiments (Figures 1–4, top). Exceptions included bacteria at the intermediate ionic strength (possible mild blocking) (Figure 3, top) and bacteria at the low flow rate (mild ripening) (Figure 4, top). Breakthrough of bacteria and microspheres occurred simultaneously with the tritium tracer (data not shown), indicating lack of retardation and differential advection.

Steady-state breakthrough plateaus decreased with increased ionic strength for both microspheres and bacteria (Figures 1 and 3, top), consistent with the observations of many previous studies (20, 21, 36–44). Steady-state breakthrough plateaus increased with increasing flow rate for both microspheres and bacteria (Figures 2 and 4, top), also consistent with many previous studies (11, 20, 21, 42, 56–59).

Retained Profiles. The magnitudes of the retained profiles of microspheres and bacteria varied oppositely to the

breakthrough plateaus (Figures 1–4, bottom), as expected from mass balance considerations (Table 1). In the case of the microspheres, hyperexponential decreases in the retained profiles were observed (Figures 1 and 2, bottom), as evidenced by the greater decrease in observed retained concentrations with distance from source relative to that expected based on simulations using a spatially constant deposition rate coefficient (Figures 1 and 2, bottom, dashed lines). The steepness of the retained microsphere profiles increased with increased ionic strength (Figure 1, bottom) and decreased with increased flow rate (Figure 2, bottom).

In contrast, the shapes of the profiles of retained bacteria varied greatly with increased ionic strength (Figure 3, bottom), displaying hyperexponential decreases at the low ionic strength (0.0038 M), whereas higher ionic strengths yielded maximum retained concentrations at locations down-gradient of the inlet. The extent of divergence from expectations is clarified by comparison of experimental results with simulations based on a spatially constant deposition rate coefficient (Figure 3, dashed lines). The peaks of mass of

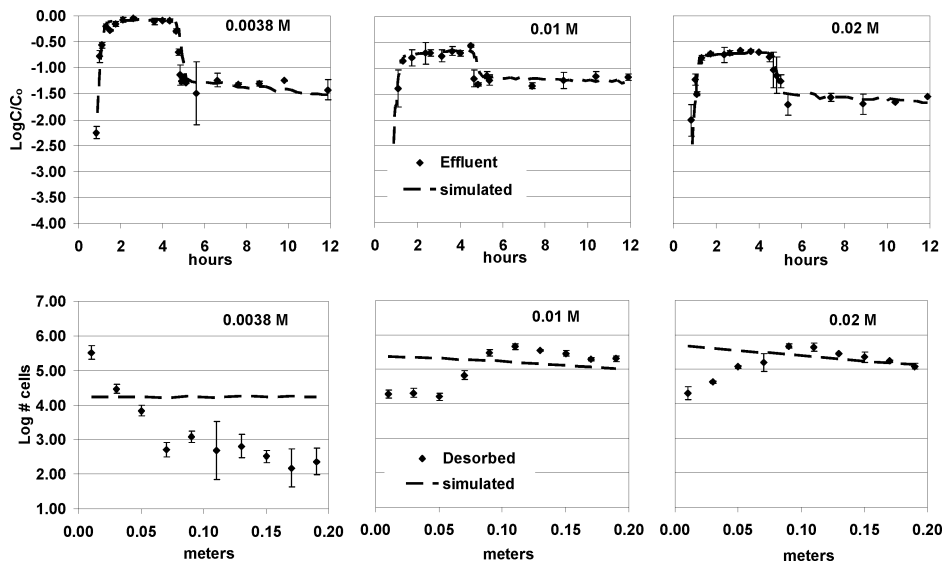


FIGURE 3. Ionic strength series for DA001 at flow rate = 4 m day^{-1} , showing effluent breakthrough-elution curves (top) and retained (desorbed) profiles (bottom). Error bars represent standard deviations in results from replicate experiments ($n = 2-4$). Simulations are shown from the particle tracking model using a single deposition rate coefficient (k_d) (dashed line).

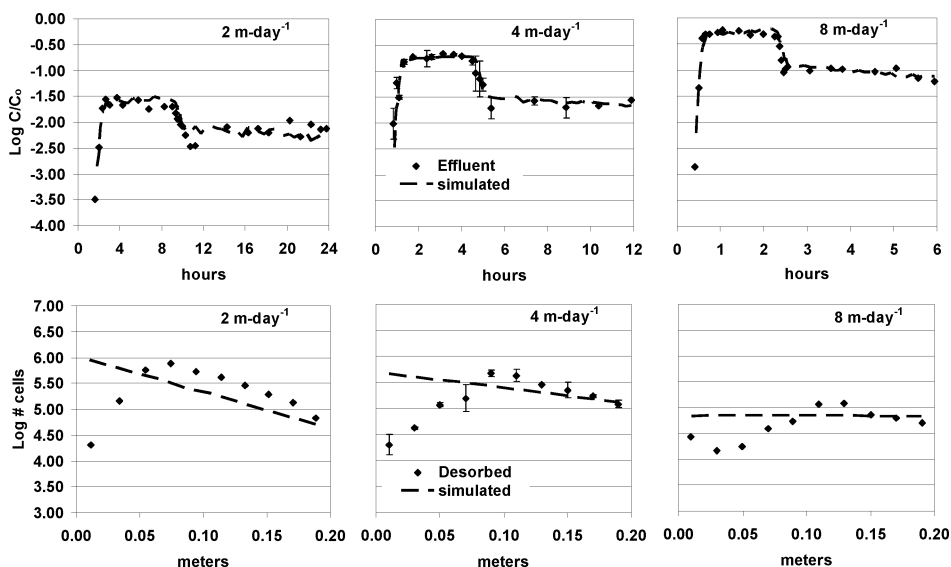


FIGURE 4. Flow rate series at ionic strength = 0.02 M , for DA001, showing effluent breakthrough-elution curves (top) and retained (desorbed) profiles (bottom). Simulations are shown from the particle tracking model using a single deposition rate coefficient (k_d) (dashed line).

the profiles of retained bacteria were located further down-gradient with increasing flow rate (Figure 4, bottom, and Figure 5).

To examine whether detachment significantly influenced the profile of retained cells, experiments were run under equivalent conditions with varying elution times. Increasing the elution time produced increasing down-gradient translation of maximum retained concentrations of cells, shown by comparison of the retained profiles after 7, 14, and 21 pore volumes (PV) elution at flow rates of 4 and 8 m day^{-1} (Figure 6, top and bottom). These findings demonstrate that detachment significantly influenced the down-gradient translation of the peak of mass of the retained profiles.

Discussion

Trends in Deposition Rate Coefficients: Comparison to Theory. The overall deposition rate coefficients (determined from breakthrough plateaus) decreased with increasing flow rate (Figures 2 and 4, top and Table 1). This trend can be evaluated relative to mass transport considerations enveloped

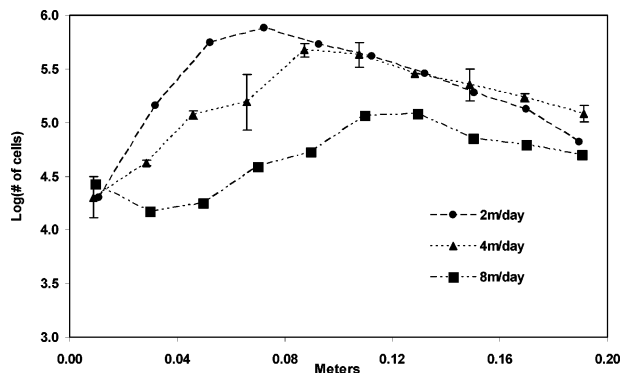


FIGURE 5. Retained profiles for DA001 at different flow rates with ionic strength = 0.02 M .

in filtration theory (1-3). Filtration theory concerns prediction of the collector efficiency (η), which represents the number of colloid-sediment collisions per number of ap-

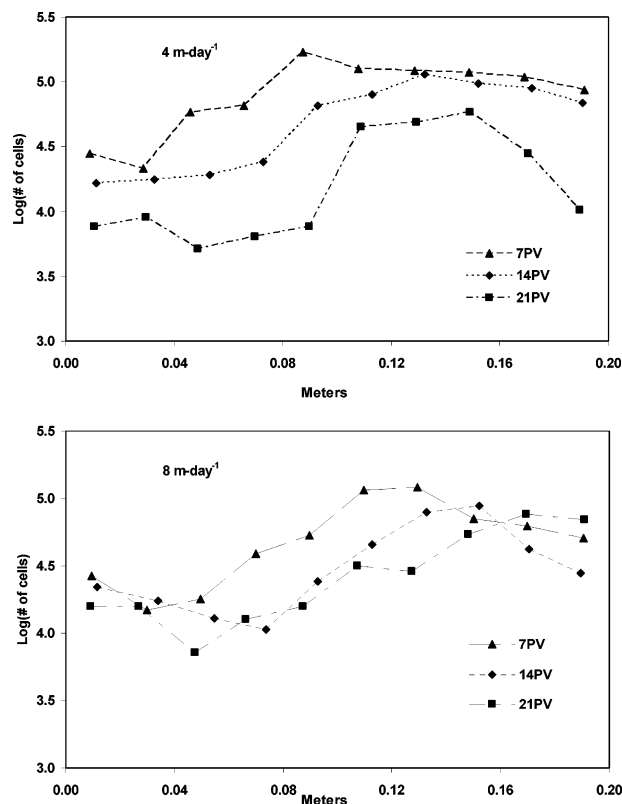


FIGURE 6. Elution duration series for DA001 at ionic strength = 0.02 M, showing retained profile for flow rate 4 m day⁻¹ (top) and 8 m day⁻¹ (bottom).

proaching colloids. Different correlation equations are available to estimate the collector efficiency, e.g. the R-T equation (2, 60–62), and the T-E equation (3). Both correlation equations evaluate the collector efficiency based on regressions of dimensionless interception, sedimentation, and diffusion parameters relative to numerical simulations of particle transport in porous media.

Both the R-T and T-E models predict a decrease in the collector efficiency with flow rate over the flow rate range examined (data not shown). The deposition rate coefficient is calculated from the collector efficiency (η) as follows

$$k_f = \frac{3}{2} \frac{(1 - \theta)}{d_c} \alpha \eta v \quad (3)$$

where θ is the sediment porosity, d_c is the collector (sediment grain) diameter, v is the fluid velocity, and α is the collision efficiency, which is the number of colloid attachments per number of collisions.

For the purpose of estimating the maximum deposition rate coefficient that is supported by mass transfer considerations, one can assume a value of the collision efficiency equal to unity. Assuming that the collision efficiency is constant with flow rate, an increase in the deposition rate coefficient with increased flow rate is predicted. The observed trends in k_f versus flow rate for microspheres and bacteria diverged from the trends expected from filtration theory (Table 1, Figure 7). Theory predicts increasing k_f with increasing flow rate, whereas observed values of k_f decreased with increasing flow rate for both microspheres and bacteria. The magnitudes of the observed deposition rate coefficients were much smaller than the theoretical maximum values, as expected.

That the deposition rate coefficient under unfavorable conditions decreased with increased flow rate (Figure 7) cannot be attributed to greater excluded areas associated

with blocking by retained colloids, since negligible blocking was observed during the majority of experiments (Figures 1–4, top). The decreased deposition rate coefficient with increased flow rate may result from increases in hydrodynamic drag, as suggested based on experiments examining microsphere transport in simple shear systems (63–65) as well as in experiments examining microsphere transport in porous media (21, 65). Note that previous experiments also have shown decreasing deposition rate coefficients with increasing flow rate (42, 56–59); however, whether these results suggest an influence of hydrodynamic drag would require comparison of the expected trend from theory, which was not performed in those studies.

Factors Governing Profile Shapes. The steady-state breakthrough plateaus of the microspheres and bacteria both decreased with increasing ionic strength (Figures 1 and 3, top), in qualitative agreement with Derjaguin-Landau-Verwey-Overbeek (DLVO) interaction energy considerations. Increasing ionic strength compressed the electrical double layer surrounding the colloids and sediment, thereby decreasing the distance over which electrostatic repulsion was significant between the colloids and the sediment surface. The decreased effective distance of electrostatic repulsion allowed greater deposition of microspheres and bacteria on the glass beads.

To develop DLVO energy profiles, the electrophoretic mobilities (EPM) of microspheres, bacteria, and crushed glass beads were measured according to Tong et al. (66). The measured EPMs yielded zeta potentials ranging from -82.7 mV to -66.1 mV for microspheres, -1.9 mV to -1.4 mV for bacteria, and -64 mV to -42 mV for crushed glass beads over an ionic strength range from 0.001 to 0.02 M at pH 6.0. The Hamaker constants were 6.60×10^{-20} J for microspheres, 6.34×10^{-20} J for crushed glass beads (67), and 5.35×10^{-20} J for bacteria based on data presented in ref 68 for this strain. The resulting DLVO energy profiles (not shown for brevity) show an electrostatic energy barrier to microsphere attachment ranging from 2416 kT at 0.006 M to 899 kT at 0.02 M and an electrostatic energy barrier to bacterial attachment ranging from 41 kT at 0.0038 M to absent at 0.02 M. A significant barrier to attachment was estimated for microspheres and bacteria at low ionic strength, yet deposition was observed. Deposition under unfavorable conditions has been well reported, and determination of its cause is beyond the scope of this paper.

The model (which utilized a constant deposition rate coefficient) was not able to simulate the shape of the retained profiles of either colloid (Figures 1–4, bottom), clearly demonstrating that the distribution of retained colloids deviated from expectations via existing filtration models. The observed hyperexponential decreases in retained microsphere concentrations with an increasing distance from the source were also observed under pH-stable conditions (20). The similarity of the retained microsphere profiles under these pH-varying and pH-stable conditions indicate that the pH increase from 6.0 to 9.4 along the flowpath was not the main cause of the hyperexponential microsphere profiles observed here. A model using a distribution of deposition rates among the microsphere “population” successfully simulated the combined breakthrough-elution curves and retained profiles under pH-stable conditions (20), indicating that distributions in interaction potentials among the microsphere “population” may account for the observed behavior.

The profiles of retained microsphere concentrations serve as a baseline for evaluating the observed profiles of retained bacteria. The very different shapes of the retained profiles observed for bacteria relative to similarly sized microspheres at high ionic strength under conditions where pH increased along the flowpath indicate that there are significant dif-

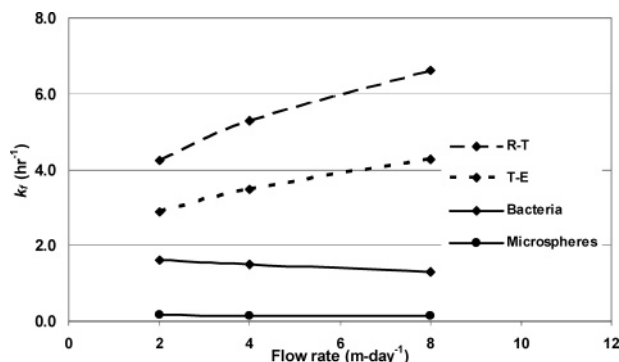


FIGURE 7. Observed and mass transport-supported deposition rate coefficients (k_r) at different flow rates. The mass transport-supported deposition rate coefficients were estimated using the R-T and T-E equations. The relatively larger effective radius of microspheres relative to bacteria increases the mass transport-supported k_r of the former by only 10% of those for the latter. The trends of mass transport-supported k_r were the same for microspheres and bacteria.

ferences in the way their respective surface chemistries respond to increased ionic strength and possibly pH.

In the bacterial transport experiments, increased ionic strength increased both the magnitude and the reversibility of deposition, since the peak concentrations of retained bacteria were translated down-gradient (Figure 3, bottom) even as overall deposition increased (Figure 3, top). These bell-shaped retained profiles have been shown scarcely in other work, for example for the protozoan *Cryptosporidium parvum* (11), and Norwalk virus (13, 18). In the former publication, the authors did not attempt to explain this distribution. In the latter publication, the authors attributed the bell-shaped retained profile to alteration of sediment surface properties (greater repulsion) at the up-gradient end of the column by dissolved organic matter and other constituents in the wastewater used in those experiments. Neither publication examined the possible role of detachment in generating the observed profiles. The observation of down-gradient maximum retained concentrations in our studies indicates that unusual water chemistries are unnecessary to yield such behavior; this behavior can be produced by simple solutions (slightly elevated NaCl concentration and elevated pH).

The increased down-gradient translation of the peak concentrations of retained bacteria with increased elution (Figure 6) demonstrated that detachment significantly influenced the down-gradient location of the profile of retained bacteria. To the knowledge of the authors, this has not been previously demonstrated in experiments. Zhang et al. (10) and Tufenkji et al. (33) demonstrated via numerical and analytical simulations that significant colloid detachment could potentially translate the retained colloids significant distances down-gradient in the column.

The effect of bacterial detachment is also manifested by the elution portion of the effluent curves, since the concentrations of bacteria observed during elution were only 1 to 1.5 orders of magnitude lower than the breakthrough plateau (Figures 3 and 4 top). In contrast, the eluted concentrations of the microspheres were 2.5 to 3 orders of magnitude lower than the plateau (Figures 1 and 2 top), and experiments examining different elution times for the microspheres showed no significant differences in the retained profiles (data not shown). These differences are captured by the simulations (fit to breakthrough-elution curves), which showed that under same ionic strength and flow condition (e.g. 0.02 M ionic strength and 4 m day⁻¹ flow rate), the fraction of attachment that was reversible (f_r) was much higher for the bacteria (0.40) than the microspheres (0.03) (Table 1). Simulated fits to the retained bacterial profiles

were not improved regardless of the values of detachment rate coefficient (k_r) and fraction of reversibility (f_r) used. Development of a model to capture the profiles of retained bacteria will first require additional understanding of the causes of the observed profiles.

Although detachment during elution was a significant contributor to the shape of the observed profiles of retained bacteria, it was not the only contributor. This is demonstrated by the nonlinearity of the degree of down-gradient translation of the peak of mass of retained bacteria relative to elution duration. For experiments performed at a flow velocity of 4 m day⁻¹, the maximum retained concentrations were located 9, 13, and 15 cm from the inlet for elution durations of 7, 14, and 21 pore volumes, respectively (Figure 6, top). If detachment during elution were the only contributor to down-gradient translation of the peak concentrations, then we would expect the maximum retained concentrations to have been located at 18 and 27 cm from the inlet for 14 and 21 pore volumes of elution, respectively. Likewise, for experiments performed at a flow velocity of 8 m day⁻¹, the maximum retained concentrations were located 13, 15, and 17 cm from the inlet for elution durations of 7, 14, and 21 pore volumes, respectively (Figure 6, bottom). Clearly, the extent of translation of the maximum retained concentrations was disproportional to the extent of elution. An experiment performed with minimum elution (1.2 pore volumes, 0.02 M ionic strength, 4 m-day⁻¹ flow rate) also showed maximum retained concentrations that were translated down-gradient from the inlet (data not shown), demonstrating that the bell-shaped profile of retained bacteria was established even before significant elution occurred.

The above results indicate that initial down-gradient translation of the peak retained bacterial concentrations was not related solely to elution but was established during injection. It is possible that detachment was enhanced during injection, e.g. in the presence of mobile cells, leading to down-gradient translation of the maximum retained concentrations during injection. Enhanced detachment during injection has been reported in the literature previously in impinging jet flow cells (69), where it was attributed to hydrodynamic collision between mobile and attached bacteria. It is also possible that increased solution pH along the flow path changed bacterial surface properties in a manner that resulted in the observed profiles. However, the zeta potentials of the bacteria ranged from -1.4 to -1.6 over the pH range from 6.0 to 9.4 at 0.02 M ionic strength, a range that is within the error of the measurement. This indicates that no significant change in the electrostatic component of the bacterial surface chemistry resulted from that pH increase. Additionally, experiments examining microsphere transport in quartz sand under pH-stable conditions also showed maximum retained microsphere concentrations down-gradient of the column inlet (21), demonstrating that these nonmonotonic retained profiles are generated in the absence of pH changes.

The reversibility of bacterial deposition at high ionic strength would suggest deposition in the secondary energy minimum, were it not for the lack of an energy barrier at high ionic strength (discussed above). It is likely that the DLVO profiles do not reflect the effects of bacterial surface polymers, which may potentially disallow deposition in the primary minimum. The prevalence of nonelectrostatic effects on deposition of bacterial strain DA001 in porous media is discussed in detail in a separate paper (66).

Implications. The fact that the peak of mass of retained cells translated down-gradient through sand at rates ranging from cm per day to cm per hour demonstrates that soil bacteria can transit the granular subsurface at rates much greater than is commonly assumed (in fact most filtration models assume complete irreversibility). The detachment-driven translation of retained bacteria demonstrated here

may contribute to the observed widespread distribution of microbes in the subsurface. The cell surface properties driving greater detachment at higher ionic strength should be investigated, as should the generality of this observation among microbes.

The soil bacterial strain examined here is not representative of all soil bacteria. *Comamonas* DA001 is a nonmotile soil bacterium isolated from a site near Oyster, VA (70). Although a number of adhesion deficient wild-type strains were isolated from Oyster, Virginia (e.g. ref 54), these strains are in the minority among the culturable soil bacterial strains (Mary DeFlaun, Geosyntec, personal communication). Nonetheless, other studies of other soil bacteria show high breakthroughs and high eluted concentrations during tailing, similar to the transport behavior of DA001, e.g. bacterial strain A0500 isolated from Savannah River Deep Subsurface Collection (71, 72), and *Klebsiella oxytoca* (59, 73). The same is true for some viruses examined in transport studies, e.g. Norwalk Virus (13).

Regardless of the extent to which the observed detachment-influenced translation of retained DA001 applies to other microbes, deviations from log-linear decreases in retained concentrations versus transport distance are widely reported for microbes and (more recently) nonbiological colloids. These deviations appear, in fact, to be the norm rather than the exception and have important implications for environmental filtration processes. Measuring a colloid deposition rate coefficient (biological or nonbiological) at a distance from a source, and extrapolating this deposition rate coefficient log-linearly to greater distances, may not be accurate, since extrapolation may greatly over- or underestimate the deposition rate coefficient at other distances. Extrapolation of deposition rate coefficient with distance may be utilized in design of environmental filtration processes such as riverbank filtration as well as determination of well-setback distances from pathogen sources.

Acknowledgments

This work was funded by a grant to William P. Johnson from the National Science Foundation Hydrologic Sciences Program (EAR 0087522).

Literature Cited

- Yao, K. M.; Habibian, M. T.; O'Melia, C. R. Water and wastewater filtration: concepts and applications. *Environ. Sci. Technol.* **1971**, *5* (11), 1105–1112.
- Rajagopalan, R.; Tien, C. Trajectory analysis of deep-bed filtration with the sphere-in-cell porous media model. *AIChE J.* **1976**, *22* (3), 523–533.
- Tufenkji, N.; Elimelech, M. Correlation equation for predicting single-collector efficiency in physicochemical filtration in saturated porous media. *Environ. Sci. Technol.* **2004**, *38* (2), 529–536.
- Albinger, O.; Biesemeyer, B. K.; Arnold, R. G.; Logan, B. E. Effect of bacterial heterogeneity on adhesion to uniform collectors by monoclonal populations. *FEMS Microbiol. Lett.* **1994**, *124* (3), 321–326.
- Baygents, J. C.; Glynn Jr, J. R.; Albinger, O.; Biesemeyer, B. K.; Ogden, K. L.; Arnold, R. G. Variation of surface charge density in monoclonal bacterial populations: implications for transport through porous media. *Environ. Sci. Technol.* **1998**, *32* (11), 1596–1603.
- Simoni, S. F.; Harms, H.; Bosma, T. N. P.; Zehnder, A. J. B. Population heterogeneity affects transport of bacteria through sand columns at low flow rates. *Environ. Sci. Technol.* **1998**, *32* (14), 2100–2105.
- Bolster, C. H.; Mills, A. L.; Hornberger, G.; Herman, J. Effect of intra-population variability on the long-distance transport of bacteria. *Ground Water* **2000**, *38* (3), 370–375.
- Harvey, R. W.; Garabedian, S. P. Use of colloid filtration theory in modeling movement of bacteria through a contaminated sandy aquifer. *Environ. Sci. Technol.* **1991**, *25* (1), 178–185.
- DeFlaun, M. F.; Murray, C. J.; Holben, M.; Scheibe, T.; Mills, A.; Ginn, T.; Griffin, T.; Majer, E.; Wilson, J. L. Preliminary observations on bacterial transport in a coastal plain aquifer. *FEMS Microbiol. Rev.* **1997**, *20* (3–4), 473–487.
- Zhang, P.; Johnson, W. P.; Scheibe, T. D.; Choi, K.; Dobbs, F. C.; Mailloux, B. J. Extended tailing of bacteria following breakthrough at the Narrow Channel Focus Area, Oyster, Virginia. *Water Resour. Res.* **2001**, *37* (11), 2687–2698.
- Harter, T.; Wagner, S.; Atwill, E. R. Colloid transport and filtration of cryptosporidium parvum in sandy soils and aquifer sediments. *Environ. Sci. Technol.* **2000**, *34* (1), 62–70.
- Gerba, C. P.; Lance, J. C. Poliovirus removal from primary and secondary sewage effluent by soil filtration. *Appl. Environ. Microbiol.* **1978**, *36* (2), 247–251.
- Redman, J. A.; Grant, S. B.; Olson, T. M.; Estes, M. K. Pathogen filtration, heterogeneity, and the potable reuse of wastewater. *Environ. Sci. Technol.* **2001**, *35* (9), 1798–1805.
- Bales, R. C.; Li, S. M.; Yeh, T. C. J.; Lenczewski, M. E.; Gerba, C. P. Bacteriophage and microsphere transport in saturated porous media: forced-gradient experiment at Borden, Ontario. *Water Resour. Res.* **1997**, *33* (4), 639–648.
- Pieper, A. P.; Ryan, J. N.; Harvey, R. W.; Amy, G. L.; Illangasekare, T. H.; Metge, D. W. Transport and recovery of bacteriophage PRD1 in a sand and gravel aquifer: effect of sewage-derived organic matter. *Environ. Sci. Technol.* **1997**, *31* (4), 1163–1170.
- DeBorde, D. C.; Woessner, W. W.; Kiley, Q. T.; Ball, P. N. Rapid transport of viruses in a flood plain aquifer. *Water Res.* **1999**, *33* (10), 2229–2238.
- Schijven, J. F.; Hoogenboezem, W.; Hassanizadeh, S. M.; Peters, J. H. Modeling removal of bacteriophages MS2 and PRD1 by dune recharge at Castricum, Netherlands. *Water Resour. Res.* **1999**, *35* (4), 1101–1111.
- Redman, J. A.; Estes, M. K.; Grant, S. B. Resolving macroscale and microscale heterogeneity in pathogen filtration. *Colloids Surf. A: Physicochem. Eng. Asp.* **2001**, *191* (1–2), 57–70.
- Bradford, S. A.; Yates, S. R.; Bettahar, M.; Simunek, J. Physical factors affecting the transport and fate of colloids in saturated porous media. *Water Resour. Res.* **2002**, *38* (12), 1327–1338.
- Li, X.; Scheibe, T. D.; Johnson, W. P. Apparent decreases in colloid deposition rate coefficient with distance of transport under unfavorable deposition conditions: a general phenomenon. *Environ. Sci. Technol.* **2004**, *38* (21), 5616–5625.
- Li, X.; Johnson, W. P. Nonmonotonic variations in deposition rate coefficients of microspheres in porous media under unfavorable deposition conditions. *Environ. Sci. Technol.* **2005**, ASAP article DOI: 10.1021/es048963b.
- Adamczyk, Z.; Siwek, B.; Szyk, L. Flow-induced surface blocking effects in adsorption of colloid particles. *J. Colloid Interface Sci.* **1995**, *174* (1), 130–141.
- Liu, D.; Johnson, P. R.; Elimelech, M. Colloid deposition dynamics in flow through porous media: role of electrolyte concentration. *Environ. Sci. Technol.* **1995**, *29* (12), 2963–2973.
- Rijnaarts, H. H. M.; Norde, W.; Bouwer, E. J.; Lyklema, J.; Zehnder, A. J. B. Bacterial deposition in porous media related to the clean bed collision efficiency and to substratum blocking by attached cells. *Environ. Sci. Technol.* **1996**, *30* (10), 2869–2876.
- Camesano, T. A.; Logan, B. E. Influence of fluid velocity and cell concentration on the transport of motile and nonmotile bacteria in porous media. *Environ. Sci. Technol.* **1998**, *32* (11), 1699–1708.
- Camesano, T. A.; Unice, K. M.; Logan, B. E. Blocking and ripening of colloids in porous media: implications for bacterial transport. *Colloid Surf. A: Physicochem. Eng. Aspects* **1999**, *160* (3), 291–307.
- Chen, G.; Strevett, K. A. Microbial deposition in porous media: a surface thermodynamic investigation. *Environ. Eng. Sci.* **2003**, *20* (3), 237–248.
- Grolimund, D.; Borkovec, M. Long-term release kinetics of colloidal particles from natural porous media. *Environ. Sci. Technol.* **1999**, *33* (22), 4054–4060.
- Grolimund, D.; Barmettler, K.; Borkovec, M. Release and transport of colloidal particles in natural porous media 2. experimental results and effects of ligands. *Water Resour. Res.* **2001**, *37* (3), 571–582.
- Ryan, J. N.; Gschwend, P. M. Effects of ionic strength and flow rate on colloid release: relating kinetics to intersurface potential energy. *J. Colloid Interface Sci.* **1994**, *164* (1), 21–34.
- El-Farhan, Y. H.; Denovio, N. M.; Herman, J. S.; Hornberger, G. M. Mobilization and transport of soil particles during infiltration experiments in an agricultural field, Shenandoah Valley, Virginia. *Environ. Sci. Technol.* **2000**, *34* (17), 3555–3559.
- Bai, R.; Tien, C. Particle detachment in deep bed filtration. *J. Colloid Interface Sci.* **1997**, *186* (2), 307–317.

- (33) Tufenkji, N.; Redman, J. A.; Elimelech, M. Interpreting deposition patterns of microbial particles in laboratory-scale column experiments. *Environ. Sci. Technol.* **2003**, *37* (3), 616–623.
- (34) Ray, C.; Melin, G.; Linsky, R. B. *Riverbank Filtration Improving Source-Water Quality*; Kluwer Academic Publishers: Netherlands, 2002; Vol. 43.
- (35) Hem, J. D. *Study and Interpretation of the Chemical Characteristics of Natural Water*, 3rd ed.; United States Government Printing Office: Washington, 1992.
- (36) Sharma, M. M.; Chang, Y. I.; Yen, T. F. Reversible and irreversible surface charge modifications of bacteria for facilitating transport through porous media. *Colloids Surf.* **1985**, *16* (2), 193–206.
- (37) Elimelech, M.; O'Melia, C. R. Kinetics of deposition of colloidal particles in porous media. *Environ. Sci. Technol.* **1990**, *24* (10), 1528–1536.
- (38) Scholl, M. A.; Mills, A. L.; Herman, J. S.; Hornberger, G. M. The influence of mineralogy and solution chemistry on the attachment of bacteria to representative aquifer materials. *J. Contam. Hydrol.* **1990**, *6* (4), 321–336.
- (39) Fontes, D. E.; Mills, A. L.; Hornberger, G. M.; Herman, J. S. Physical and chemical factors influencing transport of microorganisms through porous media. *Appl. Environ. Microb.* **1991**, *57* (9), 2473–2481.
- (40) Kinoshita, T.; Bales, R. C.; Yahya, M. T.; Gerba, C. P. Bacteria transport in a porous medium: retention of bacillus and pseudomonas on silica surfaces. *Water Res.* **1993**, *27* (8), 1295–1301.
- (41) Mills, A. L.; Herman, J. S.; Hornberger, G. M.; DeJesus, T. H. Effect of solution ionic strength and iron coating on mineral grains on the sorption of bacteria cells to quartz sand. *Appl. Environ. Microbiol.* **1994**, *60* (9), 3300–3306.
- (42) Kretzschmar, R.; Barmettler, K.; Grolimun, D.; Yan, Y. D.; Borkovec, M.; Sticher, H. Experimental determination of colloid deposition rates and collision efficiencies in natural porous media. *Water Resour. Res.* **1997**, *33* (5), 1129–1137.
- (43) Deshpande, P. A.; Shonnard, D. R. Modeling the effects of systematic variation in ionic strength on the attachment kinetics of *Pseudomonas fluorescens* UPER-1 in saturated sand columns. *Water Resour. Res.* **1999**, *35* (5), 1619–1627.
- (44) Compère, F.; Porel, G.; Delay, F. Transport and retention of clay particles in saturated porous media. Influence of ionic strength and pore velocity. *J. Contam. Hydrol.* **2001**, *49* (1–2), 1–21.
- (45) Thompson, G.; Kallay, N.; Matijević, E. Particle adhesion and removal in model systems—IX: detachment of rodlike—FeOOH particles from steel. *Chem. Eng. Sci.* **1984**, *39* (7–8), 1271–1276.
- (46) Kallay, N. T. M.; Biškup, B.; Kunjašić, I.; Matijević, E. Particle adhesion and removal in model systems; XI. kinetics of attachment and detachment for hematite-glass systems. *Colloids Surf.* **1987**, *28* (2–4), 185–197.
- (47) McEldowney, S.; Fletcher, M. Effect of pH, temperature and growth conditions on the adhesion of a gliding bacterium and three nongliding bacteria to polystyrene. *Microb. Ecol.* **1988**, *16* (2), 183–195.
- (48) Scholl, M. A.; Harvey, R. W. Laboratory investigations on the role of sediment surface and groundwater chemistry in transport of bacteria through a contaminated sandy aquifer. *Environ. Sci. Technol.* **1992**, *26* (7), 1410–1417.
- (49) Ryan, J. N.; Gschwend, P. M. Effect of solution chemistry on clay colloid release from an iron oxide-coated aquifer sand. *Environ. Sci. Technol.* **1994**, *28* (9), 1717–1726.
- (50) Bales, R. C.; Li, S.; Maguire, K. M.; Yahya, M. T.; Gerba, C. P.; Harvey, R. W. Virus and bacteria transport in a sandy aquifer, Cape Cod, MA. *Ground Water* **1995**, *33* (4), 653–661.
- (51) Jucker, B. A.; Zehnder, A. J. B.; Harms, H. Quantification of polymer interactions in bacteria adhesion. *Environ. Sci. Technol.* **1998**, *32* (19), 2909–2915.
- (52) Litton, G. M.; Olson, T. M. Colloid deposition rates on silica bed media and artifacts related to collector surface preparation methods. *Environ. Sci. Technol.* **1993**, *27* (1), 185–193.
- (53) Zhang, P.; Johnson, W. P.; Rowland, R. Bacteria tracking using ferrographic separation. *Environ. Sci. Technol.* **1999**, *33* (14), 2456–2460.
- (54) Fuller, M. E.; Mailloux, B. J.; Steger, S. H.; Hall, J. A.; Zhang, P.; Kovacic, W. P.; Vainberg, S.; Johnson, W. P.; Onstott, T. C.; DeFlaun, M. F. Application of a vital fluorescent staining method for simultaneous, near-real-time concentration monitoring of two bacterial strains in an Atlantic Coastal Plain aquifer in Oyster, Virginia. *Appl. Environ. Microbiol.* **2004**, *70* (3), 1680–1687.
- (55) Scheibe, T. D.; Wood, B. D. A particle-based model of size or anion exclusion with application to microbial transport in porous media. *Water Resour. Res.* **2003**, *39* (4), doi: 10.1029/2001WR001223.
- (56) Wollum, A. G.; Cassel, D. K. Transport of microorganisms in sand columns. *Soil. Sci. Soc. Am. J.* **1978**, *42* (1), 72–76.
- (57) Smith, M. S.; Thomas, G. W.; White, R. E.; Ritonga, D. Transport of escherichia coli through intact and disturbed soil columns. *J. Environ. Qual.* **1985**, *14* (1), 87–91.
- (58) Tan, Y.; Gannon, J. T.; Baveye, P.; Alexander, M. Transport of bacteria in an aquifer sand: experiments and model simulations. *Water Resour. Res.* **1994**, *30* (12), 3243–3252.
- (59) Hendry, M. J.; Lawrence, J. R.; Maloszewski, P. Effects of velocity on the transport of two bacteria through saturated sand. *Ground Water* **1999**, *37* (1), 103–112.
- (60) Rajagopalan, R.; Tien, C.; Pfeffer, R.; Tardos, G. Letter to the editor. *AIChE J.* **1982**, *28* (5), 871–872.
- (61) Tien, C. *Granular filtration of aerosols and hydrosols*; Mass, 1989; Vol. 1.
- (62) Logan, B. E.; Jewett, D. G.; Arnold, R. G.; Bouwer, E. J.; O'Melia, C. R. Clarification of clean-bed filtration models. *J. Environ. Eng.* **1995**, *121* (12), 869–873.
- (63) Meinders, J. M.; Busscher, H. J. Adsorption and desorption of colloidal particles on glass in a parallel plate flow chamber—Influence of ionic strength and shear rate. *Colloid Polymer Sci.* **1994**, *272* (4), 478–486.
- (64) Varennes, S.; van de Ven, T. G. M. Deposition and detachment of latex particles at glass surfaces exposed to flow. *Phys. Chem. Hydrodyn.* **1987**, *9* (3–4), 537–559.
- (65) Brow, C.; Li, X.; Rička, J.; Johnson, W. P. Comparison of microsphere deposition in porous media versus simple shear systems. *Colloids Surf. A: Physicochem. Eng. Aspects* **2005**, *253* (1–3), 125–136. press.
- (66) Tong, M.; Camesano, T. A.; Johnson, W. P. Spatial variation in deposition rate coefficients of an adhesion deficient bacterial strain in quartz sand. *Environ. Sci. Technol.* **2004**, in revision.
- (67) Bergendahl, J.; Grasso, D. Prediction of colloidal detachment in a model porous media: thermodynamics. *AIChE J.* **1999**, *45* (3), 475–484.
- (68) Dong, H.; Onstott, T. C.; Ko, C.; Hollingsworth, A. D.; Brown, D. G.; Mailloux, B. J. Theoretical prediction of collision efficiency between adhesion-deficient bacteria and sediment grain surface. *Colloids Surf. B: Biointerfaces* **2002**, *24* (3–4), 229–245.
- (69) Meinders, J. M.; Busscher, H. J. Influence of interparticle interactions on blocked areas and desorption during particle deposition to glass in a parallel plate flow chamber. *Langmuir* **1995**, *11* (1), 327–333.
- (70) Fuller, M. E.; Sterger, S. H.; Rothmel, R. T.; Mailloux, B. J.; Hall, J. A.; Onstott, T. C.; Frederickson, J. K.; Balkwill, D. L.; DeFlaun, M. F. Development of a vital fluorescent staining method for monitoring bacterial transport in subsurface environments. *Appl. Environ. Microbiol.* **2000**, *66* (10), 4486–4496.
- (71) Johnson, W. P.; Blue, K. A.; Logan, B. E.; Arnold, R. G. Modeling bacteria detachment during transport through porous media as a residence-time-dependent process. *Water Resour. Res.* **1995**, *31* (11), 2649–2658.
- (72) McCaulou, D. R.; Bales, R. C.; Arnold, R. G. Effect of temperature-controlled motility on transport of bacteria and microspheres through saturated sediment. *Water Resour. Res.* **1995**, *31* (2), 271–280.
- (73) Hendry, M. J.; Lawrence, J. R.; Maloszewski, P. The role of sorption in the transport of *Klebsiella oxytoca* through saturated silica sand. *Ground Water* **1997**, *35* (4), 574–584.

Received for review June 29, 2004. Revised manuscript received January 17, 2005. Accepted January 21, 2005.

ES049013T